The Key Role of Solvation Dynamics in Intramolecular Electron Transfer: Time-Resolved Photophysics of Crystal Violet Lactone

Uli Schmidhammer,[§,†] Uwe Megerle,[†] Stefan Lochbrunner,[||,†] Eberhard Riedle,*[,†] and Jerzy Karpiuk*[,‡]

Lehrstuhl für BioMolekulare Optik, Ludwig-Maximilians-Universität (LMU), Oettingenstr. 67, 80538 München, Germany, and Institute of Physical Chemistry, Polish Academy of Sciences, Kasprzaka 44/52, 01-224 Warsaw, Poland

Received: January 29, 2008; Revised Manuscript Received: June 7, 2008

The intramolecular electron-transfer reaction in crystal violet lactone in polar aprotic solvents is studied with femtosecond transient absorption spectroscopy. The initially excited charge transfer state ^1CT_A is rapidly converted into a highly polar charge transfer state ^1CT_B. This ultrafast electron transfer is seen as a solvent-dependent dual fluorescence in steady-state spectra. We find that the electron-transfer process can be followed by a change from a double-peaked transient absorption spectrum to a single-peak one in the low picosecond range. The transient absorption kinetic curves are multiexponential, and the fitted time constants are solvent dependent but do not reproduce the known solvation times. For 6-dimethylaminophthalide, the optically active constituent of crystal violet lactone, only a small temporal evolution of the spectra is found. To explain these findings, we present a model that invokes a time-dependent electron-transfer rate. The rate is determined by the instantaneous separation of the two charge-transfer states. Because of their differing dipole moments, they are dynamically lowered to a different extent by the solvation. When they temporarily become isoenergetic, equal forward and backward transfer rates are reached. The intrinsic electron-transfer ($^1CT_A \rightarrow {}^1CT_B$) reaction is probably as fast as that in the structurally analogous malachite green lactone (on the 100 fs time scale). The key element for the dynamics is therefore its control by the solvent, which changes the relative energetics of the two states during the solvation process. With further stabilization of the more polar state, the final equilibrium in state population is reached.

I. Introduction

Excited molecules in solution and their chemical reactions are often considerably affected by the interaction with the environment. The dynamical behavior of the solvent molecules can lead to significant charge redistribution and the population of charge-transfer (CT) states that are inaccessible in the absence of solute−solvent interactions. The dynamics of such solvent-controlled electron-transfer (ET) processes reflects the interplay between intramolecular and solvation dynamics. Generally, a two-dimensional reaction coordinate is used in the description to include both the vibronic couplings and the solvent degrees of freedom.[1] The kinetics of solvent-controlled ET processes has been extensively studied theoretically,[2,3] but the existing body of time-dependent studies demonstrating the dynamic solvent control of ET[3−11] still leaves important fundamental questions open. In this paper, we want to experimentally clarify the impact of solvation on the ET dynamics and how the progress of the solvation influences the ET.

So far, little experimental effort has been made on separating the two components of the reaction coordinate and exploring the mechanism of solvent control. This is a consequence of focusing on a limited number of molecular systems and of inherent characteristics of the ET processes in these systems. A specific ET process to be used to visualize the solvent control should be driven by a strong enough electronic coupling such that for suitable energetics of the donor and acceptor levels, the ET process will be much faster than the response of the solvent. To the best of our knowledge, molecular systems with documented strong coupling and suitable influence of the solvent on the energetics have not yet been described in the literature.

Early investigations linked the ET processes to the longitudinal dielectric relaxation time (τ_L) of the solvent.[2,12] When ET reactions faster than τ_L were reported,[13,14] it became clear that the rate of both intramolecular[15−20] and intermolecular[21,22] ET processes can by far exceed τ_L. Extremely rapid ET processes with predicted rates up to 10^{14} s^{-1} have been proposed,[23,24] but until now experimental reports on intramolecular ET on this time scale are still very scarce.[17−20] Recently, we approached this limit by showing that intramolecular ET in phenolphthalein is accomplished within 50 fs,[25] in accord with a few other reports presenting sub-100 fs ET processes.[26,27]

The understanding of solvation dynamics[28−33] and the effects it may exert on the CT processes relies heavily on time-resolved solvation data.[34] The solvation occurs on multiple time scales ranging from less than 100 fs to several picoseconds.[29,30,34] The studies of the solvent response and of the mechanism of solvation used a variety of simple dyes and experiments based on time-dependent Stokes-shift measurements.[34] This method is believed to provide a linear image of the solvation process; the application is, however, limited to highly fluorescing probe molecules, and it is based on a number of assumptions[34] such

* Corresponding authors. E-mail: riedle@physik.uni-muenchen.de and karpiuk@ichf.edu.pl.
† Ludwig-Maximilians-Universität.
‡ Polish Academy of Sciences.
§ Present address: Laboratoire de Chimie Physique, ELVSE, UMR8000, CNRS, Université Paris-Sud, bâtiment 349, 91405 Orsay cedex, France.
|| Present address: Institut für Physik, Universität Rostock, Universitätsplatz 3, 18055 Rostock, Germany.

10.1021/jp800863u CCC: $40.75
Published on Web 08/21/2008

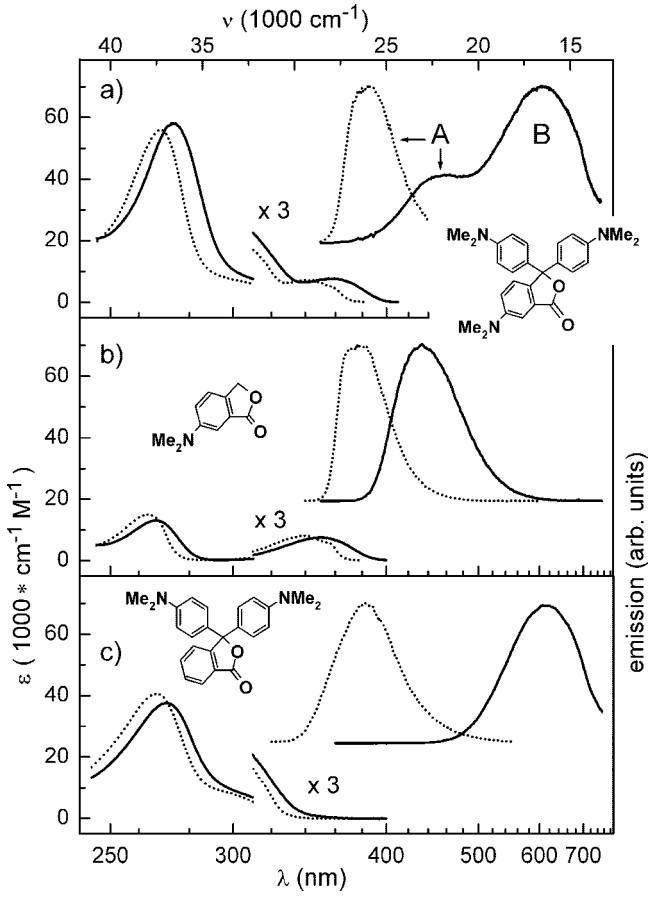

Figure 1. Steady-state absorption and emission spectra of (a) CVL, (b) 6-DMAPd, and (c) MGL in ACN (solid lines) and *n*-hexane (dotted lines). All solutions were excited in the first absorption band (λ_{exc} = 353 nm for CVL and 6-DMAPd, λ_{exc} = 310 nm for MGL). Note that the dual fluorescence spectrum (bands A and B) of CVL in ACN is approximately the sum of the spectra of 6-DMAPd and MGL.

as the absence of electronic relaxation in the probe molecule and vibrational relaxation being much faster than solvation.

Up to now, experimental investigations of the dynamical solvent effect on the reaction dynamics have focused on small organic molecules,[4,6,7,9,26,35] metal complexes,[18,36,37] and CT to solvent states.[38] To clearly separate the influence of the solvation from the intramolecular properties that determine the speed of ET, molecules are needed which allow ET under favorable conditions faster than the solvation time scale. A very promising class of molecules in this context are lactone forms of triarylmethane dyes (LTAM), well-defined molecular systems with donor and acceptor units built around a tetrahedral carbon atom. Such an arrangement of donor and acceptor results in a weak donor−acceptor electronic coupling in the ground state so that the absorption transitions in LTAMs in the lower energy region are localized on their structural subunits. Moreover, an appropriate substitution of the donor or acceptor subunits allows for tuning of the ET process and even for observation of qualitatively new phenomena such as, for instance, the newly discovered population of two polar excited states displaying dual fluorescence in crystal violet lactone (CVL).[39]

CVL is a colorless lactone derivative of the triarylmethane dye crystal violet. The CVL molecule is composed of two dimethylaniline (DMA) groups attached via a tetrahedral carbon atom to 6-dimethylaminophthalide (6-DMAPd) at position 3 (see Figure 1). The lowest state populated in absorption is localized on the 6-DMAPd moiety. In moderately and highly polar aprotic solvents, CVL emits fluorescence from two different polar excited states: (i) the optically populated, moderately polar state localized on 6-DMAPd and (ii) a highly polar CT state populated upon ET from one of the DMA groups to the lactone ring of the 6-DMAPd subunit.[39]

For LTAMs with a CT state approximately degenerate to or below any locally excited state,[40] we have found that the ET proceeds faster than the ultrafast solvation. In malachite green lactone (MGL), it takes 150 fs upon excitation to the S_2 state, and in phenolphthalein, it takes 50 fs upon excitation to the S_1 state.[25] Here, we study the dynamics of CVL, which is the dimethylamino derivative of MGL (see Figure 1). Contrary to MGL, the optically excited state of CVL lies below the highly polar CT state, and the latter becomes accessible only after sufficient solvation. From steady-state spectroscopy, we have argued that the kinetics in CVL involves two processes: lowering the energy of the CT state by solvation and the actual intramolecular ET. Based on the analogy with MGL, one expects that the latter occurs on the time scale of 100 fs once the CT state becomes energetically accessible. Observation of an ET product on the ultrafast time scale will give a direct proof of the suggested model and determine the actual speed of the process.

It has been shown by low-temperature studies in MGL that possible large-amplitude motions of the DMA groups do not have any significant effect on the charge separation.[41] This conclusion is also supported by investigations on the structurally related but rigid lactone form of rhodamine 101.[42] Here, twisting motions are even impossible for promoting the highly efficient ET. Because of the very similar nature of the CT_B state in CVL and the CT state in MGL, we extend this conclusion to CVL. As a consequence, a possible motion of the DMA groups should also not be relevant for the ET dynamics in CVL.

The present paper reports a femtosecond pump−probe study of the photoinduced ET in CVL and in 6-DMAPd in polar aprotic solvents with differing dielectric response. The time evolution of the transient absorption (TA) allows us to identify the emerging electronic structure and to follow the kinetics of the transformation. The excited-state dynamics of CVL are compared with those of the substructures of CVL (6-DMAPd and MGL), and the results lead to a detailed picture of the CT process in CVL and its dependence on the stage of solvation.

II. Experimental Section

CVL (Aldrich) was crystallized twice from acetone. MGL was synthesized as described by Fischer[43] and subsequently repeatedly recrystallized from 1-propanol. 6-DMAPd was synthesized as described by Stanetty et al.[44] and purified by repeated crystallization from methanol. The solvents *n*-hexane, butyl ether, ethyl acetate, acetonitrile (ACN), and dimethylsulfoxide (DMSO) were of spectroscopic quality. Propylene carbonate (PC) was of analytical purity grade. All measurements were performed at room temperature.

For fluorescence measurements, the optical densities of the samples were 0.1−0.15 at the excitation wavelengths (1 cm layer). For the femtosecond experiments, the concentrations of CVL and 6-DMAPd were chosen such that the optical density of a 1 mm layer was 0.3−0.5. Absorption spectra were recorded with Shimadzu UV 3100 and Perkin-Elmer Lambda 19 spectrophotometers, and the fluorescence spectra were measured with an Edinburgh Analytical Instruments FS900 spectrofluorimeter. The raw fluorescence spectra were corrected by subtraction of the background due to the solvent and for the instrumental response. The fluorescence spectra were recorded as a function

of wavelength and subsequently multiplied by a factor λ^2 to convert counts per wavelength interval into counts per wavenumber interval. The absorption spectra of CVL and 6-DMAPd did not change during the laser measurements, which proves the photostability of both compounds under the experimental conditions of this work.

The femtosecond TA measurements were performed with a broadband pump−probe setup. A Ti:sapphire amplifier system (CPA 2001; Clark-MXR) was used to pump a two-stage noncollinear optical parametric amplifier (NOPA) delivering ~7 μJ pulses at 740 nm. Frequency doubling in a 140 μm BBO crystal yielded 370 nm pump pulses that were compressed to ~ 80 fs. By focusing another part of the Ti:sapphire laser (typically 1 μJ) into a rotating CaF_2 disk (4 mm thickness), a supercontinuum was generated and used as probe. The fundamental wavelength (775 nm) was blocked by a dielectric mirror with high transmittance (>80%) between 300 and 700 nm and high reflectance around 800 nm. The pump and the probe pulses were focused into the sample with spherical mirrors. After the interaction in the sample, the probe beam was dispersed with a motorized monochromator with a spectral resolution of 6 nm and detected with a photodiode module (PDI-400−1−P-UV; Becker&Hickl GmbH). The temporal dispersion of the continuum due to the filter, the entrance window of the fused silica cell, and the sample amounted to about 800 fs between 350 and 700 nm. It was corrected while measuring the transient spectra. The temporal resolution was determined to be better than 300 fs. The pump energy was limited to about 270 nJ per pulse to avoid nonlinear effects such as multiphoton ionization of the solvent. The polarizations of the pump and probe pulses were set to the magic angle.

III. Results

III.1. Ground-State Absorption and Solvent-Dependent Emission of CVL. Steady-state absorption and fluorescence spectra of CVL, MGL, and 6-DMAPd in *n*-hexane and in ACN are shown in Figure 1. The absorption spectra did not show any absorption in the visible, both before and after the fluorescence and TA measurements, indicating that only the colorless lactone forms and no colored ionic forms (e.g., crystal violet cation, CV^+,[45] or malachite green cation, MG^+ [46]) were present. The spectrum of CVL at wavelengths above 250 nm is a superposition of the contributions from the *N*,*N*′-dimethylaniline and 6-DMAPd moieties in both solvents. Such additivity of absorption transitions localized on structural parts of the molecule was earlier reported for MGL[47] and for other leuco forms of triarylmethanes[48] and was explained by weak ground-state conjugation of the chromophores forming the molecule. The lowest-energy, low-intensity absorption band shows (both in CVL and in 6-DMAPd) a red shift with increasing solvent polarity (for CVL, 1600 cm^{-1} from hexane to DMSO) and has been ascribed to a CT transition localized on 6-DMAPd.[39,49] This means that only the 6-DMAPd subunit of CVL is excited in the pump−probe experiments with 370 nm excitation.

Depending on the solvent polarity, CVL emits in aprotic solvents at room temperature single (A band, low polar solvents) or dual (A and B bands, medium and highly polar solvents) fluorescence (see Figure 1a). Strong solvatochromic shifts of both fluorescence bands prove a significant charge redistribution in both emitting states, hereinafter referred to as ^1CT_A and ^1CT_B. A comparison with 6-DMAPd and MGL shows that the A band emanates from a polar excited state localized within the 6-DMAPd subunit (^1CT_A, μ_e = 10.7 D), and the B band emanates from a highly polar state (^1CT_B, μ_e = 25.2 D) formed after full ET from one of the dimethylaniline groups to the 6-DMAPd moiety.[39] Because of the symmetry and spiro-like architecture of CVL, the two dimethylaniline groups are equivalent.

The fluorescence spectra of 6-DMAPd and MGL consist of a single band each (Figure 1b,c) that shows pronounced red shifts with increasing solvent polarity. A comparison of the spectral position and width of the fluorescence band of 6-DMAPd with the short wavelength A band of CVL strongly suggests that in both molecules, the emission comes from the same chromophore. The approximate mirror symmetry of the absorption and emission spectra[50] of CVL in low polar solvents proves that both the first absorption band and the fluorescence band belong to the same electronic transition. The excited-state dipole moment of 6-DMAPd is significantly larger (μ_e = 11.2 D)[51] than that in the S_0 state (μ_g = 6.55 D) and indicates sizable charge redistribution upon excitation. The angular displacement of the $\vec{\mu}_e$ vector against $\vec{\mu}_g$ (34.8°) indicates CT from the dimethylamino group toward the meta position of the benzene ring in 6-DMAPd.[49]

The B band in CVL is very similar to the fluorescence band of MGL in terms of half-width, spectral position, and solvatochromic shift of the fluorescence maximum (see Figure 1). The spectral similarity implies that these two bands come from excited states with very similar electronic structures. The fluorescence of MGL shows a very large Stokes shift (exceeding 16 000 cm^{-1} in DMSO) and a strong solvatochromic effect and has been assigned to emanate from a highly polar CT state (μ_e = 25.0 D) with an electron transferred from the dimethylaminophenyl ring to the phthalide moiety.[41] In light of the analogies between CVL and MGL and equal dipole moments in the CT state of MGL and the ^1CT_B state of CVL, the same conclusion holds for CVL, and the long-wavelength fluorescence is assigned to a radiative back ET from the ^1CT_B state to the ground state.[39]

III.2. Solvation Equilibrated TA of CVL and 6-DMAPd. Time-resolved absorption spectra of CVL and 6-DMAPd after excitation with 370 nm pulses were measured between 380 and 700 nm. Even at the short wavelength edge of this range and for the most polar solvents, the ground-state absorption of all investigated molecules is negligible compared to the excited-state absorption. For delay times larger than 100 ps, no changes of the spectral shape and positions were found. The eventual decrease of the TA signal in the nanosecond range is due to the electronic relaxation back to the ground state. The TA spectra of CVL in ACN and in butyl ether at a delay time of 100 ps (Figure 2a) agree well with those reported for a nanosecond TA study[39] and prove that the absorbing species are already the products of a solvent-dependent excited-state process occurring on a time scale shorter than 100 ps. The spectra show only TA throughout the visible and no indication of stimulated emission. This is also true for all other transient spectra reported below. At first sight, this is surprising because the fluorescence of the molecules is also observed in the visible (see Figure 1). The first absorption band of CVL (and also 6-DMAPd) is quite weak ($\varepsilon \approx 2500$ cm^{-1} M^{-1}) because of its CT character. The electronic transition corresponding to the A band of the fluorescence can be expected to be equally weak, and by comparison, we find the same to be true for the B band. This means that the stimulated emission signal will also be weak. In contrast, any transition from the excited state to higher electronic states is most likely much stronger, and the resulting excited-state absorption will totally mask the weak stimulated emission signal.

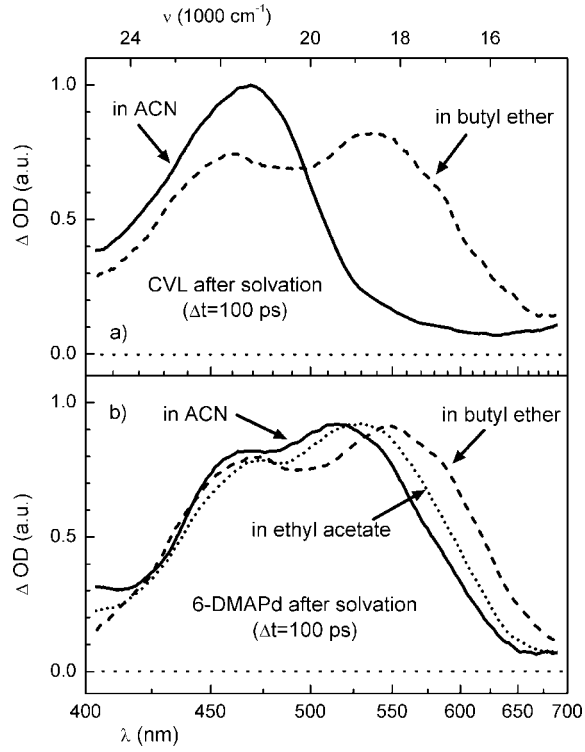

Figure 2. TA spectra of (a) CVL and (b) 6-DMAPd in low (butyl ether), intermediate (ethyl acetate), and high polarity (ACN) solvents. The spectra were recorded for λ_{exc}=370 nm and at a 100 ps delay. At this time, all solvation and ET processes are completed, and no further change of the spectral shape and positions can be found.

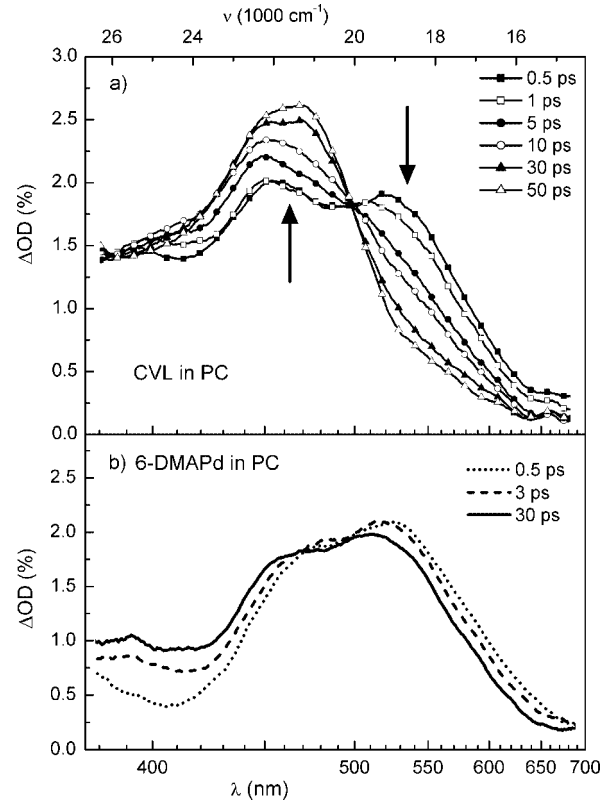

Figure 3. TA spectra recorded at various delay times after 370 nm excitation of (a) CVL and (b) 6-DMAPd in PC. Note the isosbestic point found for the CVL spectra.

The TA spectrum of CVL in the low polarity butyl ether consists of two absorption bands with maxima at 460 and 540 nm. Because the steady-state emission spectrum of CVL in butyl ether (spectrum not shown) does not show dual-band character or a significant Stokes shift,[39] it can be concluded that after 100 ps, the system is still in the optically excited state (^1CT_A). The observation of the double-peak TA spectrum can therefore serve as indication that CVL is in the ^1CT_A state. Additional strong support for this proposition comes from the close similarity of the CVL spectrum with the TA spectrum of 6-DMAPd (see Figure 2b). In 6-DMAPd, no additional CT process can occur after the optical excitation, and the same holds for CVL in low polarity solvents. Only a weak shift of the double peaked TA spectrum with the solvent polarity is observed for 6-DMAPd. This shows that the influence of solvation on the TA spectrum is weak for a given electronic state.

The TA spectrum recorded for CVL in the highly polar ACN differs strongly and consists of a single large band with a maximum at 470 nm. We suggest to take this spectral signature as indication that ET has occurred and the ^1CT_B state is populated. The TA band of CVL in ACN at 100 ps agrees very well with the absorption band of the radical cation of DMA,[52] which proves the radical ion pair nature of the ^1CT_B state[39] responsible for the single-peak TA spectrum.

The strong dependence of the TA spectra on solvent polarity indicates that in low polarity solvents, the photophysics of CVL is confined to the 6-DMAPd subunit, whereas in moderately and highly polar ones, the product of a fast excited-state ET process is observed on the 100 ps time scale.

III.3. Femtosecond Transient Spectra and Kinetics in Polar Solvents. In the preceding sections, we identified signatures of the TA spectra that can serve as indications for the electronic state that CVL and 6-DMAPd occupy. We now turn to the temporal evolution of the systems between the optical excitation and the quasi-equilibrium achieved after 100 ps.

TA spectra of CVL and 6-DMAPd in the highly polar PC are shown in Figure 3. For 6-DMAPd, only extremely small shifts are found (Figure 3b) that can be assigned to solvation of the only accessible CT state and possibly some intramolecular vibrational relaxation (IVR). In contrast, the spectra for CVL change from the double-peaked initial form to the single-peaked form typical for the ^1CT_B state. The change reflects the direct observation of the ultrafast transition from the optically excited ^1CT_A state to the ^1CT_B state. The very pronounced isosbestic point signals the direct interconversion of only two participating states.

The temporal evolution can best be investigated at the maximum of the ^1CT_B peak and in the red slope of the ^1CT_A spectrum. The TA kinetic traces shown in Figure 4a demonstrate this point. At 470 nm, the optical density increases and signals the developing population of the ^1CT_B state, whereas the optical density decreases at 580 nm and signals the decay of the ^1CT_A population.

To quantify the temporal evolution, we have fitted the experimental curves with biexponential functions and a constant signal to account for the long time quasi-equilibrium. The time constants represent a parametrization of the observed kinetic traces and cannot be directly identified with solvation times (see discussion below).

For 6-DMAPd also, a slight rise of the TA signal at short wavelengths and a slight decrease at long wavelengths is found (Figure 4b). These curves can be fitted with single-exponential functions. The time constants give an indication for the solvation of the only accessible CT state and possibly IVR.

In ACN, each compound displays a behavior of the TA very similar to that found for PC (see Figure 5). Again, an isosbestic

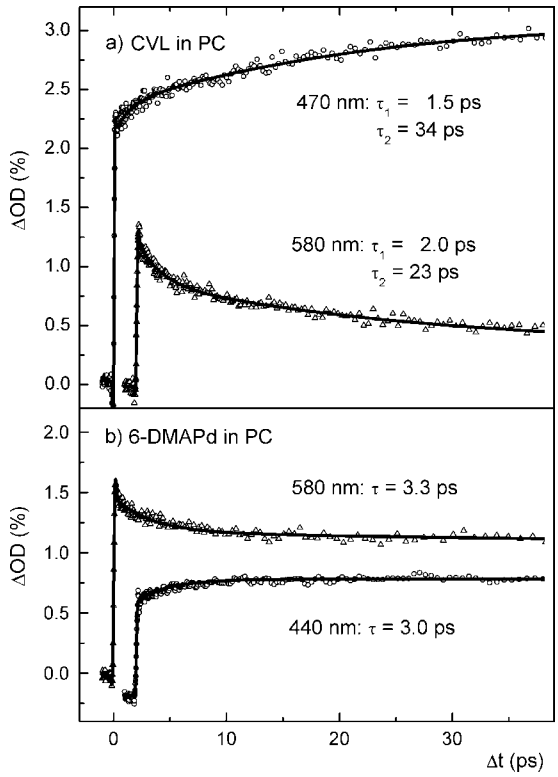

Figure 4. TA kinetic curves for (a) CVL and (b) 6-DMAPd in PC after excitation at 370 nm. For better visibility, one curve in each panel is slightly shifted. The solid lines are double-exponential functions (for CVL) and single-exponential functions (for 6-DMAPd) fitted to the data. The sharp peak observed at $t = 0$ is due to a coherent artifact.

point is observed for the CVL spectra and indicates the straight population transfer between only two states. A closer look shows that the temporal evolution in ACN is faster than that in PC. This tendency matches the well-documented faster solvation of ACN.[34]

The temporal evolution of the TA signals of CVL in ACN was monitored at 470 and 550 nm (see Figure 6). Again, at the blue maximum of the single-peaked TA spectrum, a strong rise is found, and in the red slope, a corresponding decrease is found. The fits render a nearly single-exponential behavior, but a close inspection also reveals a weak contribution in the range of hundreds of femtoseconds. The slow component is about three times faster than that in PC.

All fitted parameters are collected in Table 1. For each time constant, the associated preexponential factor a_i is given in addition. The latter values are normalized to the initial amplitude a_0 of the signal after the optical excitation.[53] In addition to the solvents ACN and PC explicitly shown in this work, we also measured the ET dynamics in DMSO and include the obtained exponential constants in Table 1.

IV. Discussion and Modeling

IV.1. Observation of the ET by TA. The established method for the characterization of ET processes is the analysis of the changes in the emission spectrum with solvent polarity and time. From a large Stokes shift, a strong change of the dipole moment in the electronically excited state is typically deduced. To obtain a quantitative understanding of the excited-state dynamics, however, the solvation-dependent rise of the ground-state energy has to be considered, and the observed spectral shift cannot be simply ascribed to a lowering of the excited state. Moreover, the concurrence of solvation and ET processes cause a high degree of complexity.

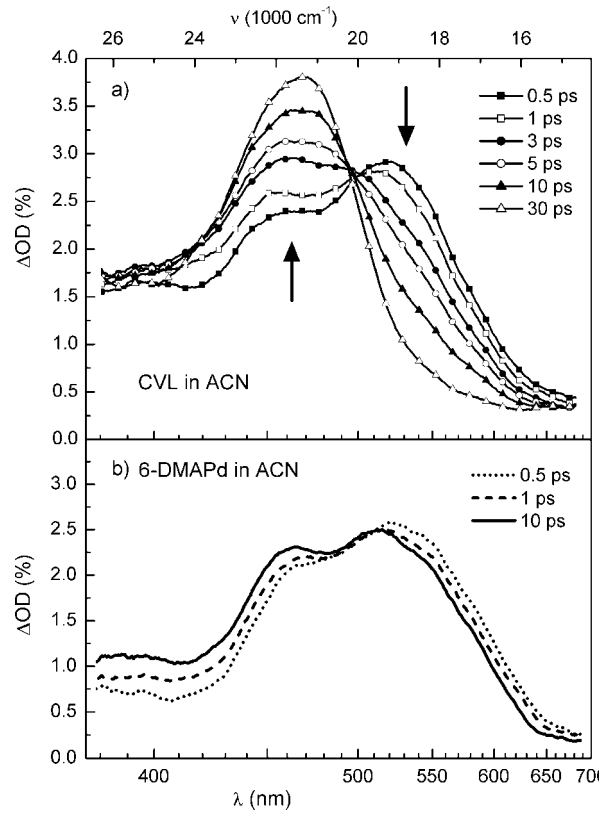

Figure 5. TA spectra recorded at various delay times after 370 nm excitation of (a) CVL and (b) 6-DMAPd in ACN. Note the isosbestic point found for the CVL spectra. Compared to Figure 3, shorter times are shown, reflecting the faster dynamics in ACN.

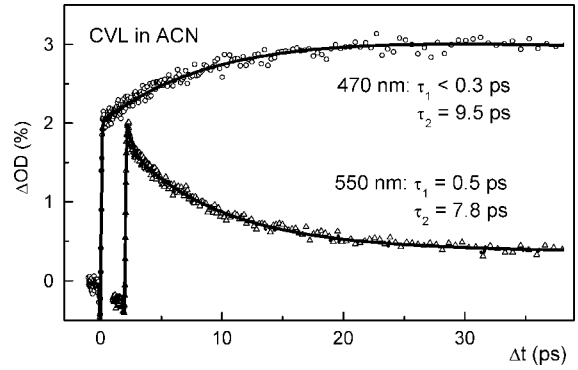

Figure 6. TA kinetic curves of CVL in ACN after excitation at 370 nm. For better visibility, the curve at 550 nm is slightly shifted.

In this work, we use the TA spectrum to analyze the ultrafast ET process. The recording of the time-resolved emission is quite difficult or even impossible for molecules with a weak electronic transition from the considered excited state to the ground state. Such a weak transition is quite common for a CT state with its largely changed electronic wave function. On the contrary, there is most likely some higher electronic state with a good transition strength, and in the investigated CVL molecule, such a transition is actually found in the experimentally accessible spectral range. The fact that neither the polarity of the solvent nor the solvation changes the TA bands significantly allows for the straightforward interpretation of the observed changes as ET dynamics. The TA measurement also does not suffer from the decrease of emission yield with the decreasing energy gap between the solvated CT state and the ground state for strongly polar solvents.[39]

TABLE 1: Time Constants Obtained from Fitting of Kinetic Curves of CVL and 6-DMAPd in ACN, DMSO, and PC[a]

CVL		6-DMAPd		
acetonitrile				
τ_1 (ps)	a_1/a_0	τ_1 (ps)	a_1/a_0	
<0.3		0.7	−0.55	rise
0.5	0.16	1.0	0.15	decay
τ_2 (ps)	a_2/a_0	τ_2 (ps)	a_2/a_0	
9.5	−0.61			rise
7.8	0.55			decay
dimethylsulfoxide				
τ_1 (ps)	a_1/a_0	τ_1 (ps)	a_1/a_0	
1.4	−0.12	1.8	−0.13	rise
1.4	0.19	1.7	0.12	decay
τ_2 (ps)	a_2/a_0	τ_2 (ps)	a_2/a_0	
12	−0.25	6.1	−0.08	rise
15	0.31	7.5	0.05	decay
propylene carbonate				
τ_1 (ps)	a_1/a_0	τ_1 (ps)	a_1/a_0	
1.5	−0.11	3.0	−0.24	rise
2.0	0.28	3.3	0.20	decay
τ_2 (ps)	a_2/a_0	τ_2 (ps)	a_2/a_0	
34	−0.61			rise
23	0.42			decay

[a] A rise of the TA is found at short wavelengths and a decay at long wavelengths. The amplitudes a_1 and a_2 of the two exponential contributions are given relative to the signal amplitude a_0 directly after the excitation pulse.

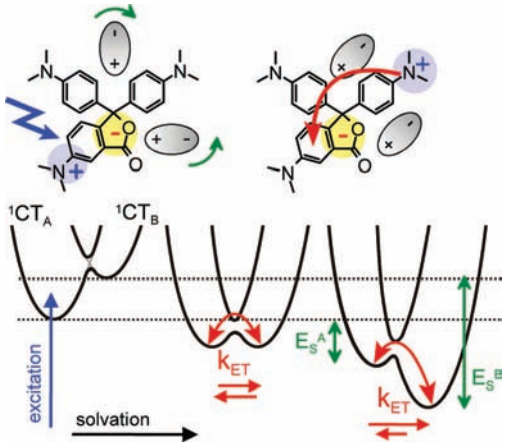

Figure 7. Snapshots of the excited energy levels of CVL during solvation. Left: after optical excitation. Middle: during solvation of the molecule, when the ^1CT_A and ^1CT_B state are in energetic resonance. Right: when solvation is completed. k_{ET} is the rate of ET. The molecular cartoons depict the charge reorganization, and the red arrows refer to the transfer of the electron.

IV.2. Solvent-Dependent Temporal Evolution of the ET. From the time-dependent TA spectra of CVL reported in Section III, we directly get information on the depopulation of the optically excited ^1CT_A state and the population of the ^1CT_B state. The isosbestic point observed for all solvents (compare Figures 3 and 5) proves that there is no additional state involved in the transfer. The rise of the TA signal at the maximum of the single-peaked band assigned to the ^1CT_B state and the decrease in the red wing that best monitors the ^1CT_A state occur with the same time constants for each solvent within the experimental accuracy.

Our fit parameters (Table 1) are in the subpicosecond and picosecond range just as the solvation times reported by Maroncelli and co-workers.[34] There is, however, no close match between these measured solvation times and our fitted time constants for the ET in CVL. What we do find is a reasonable correlation with the dielectric response and solvation energy as well as the viscosity as we go from ACN to DMSO and PC. We also find a similar trend for the solvation of 6-DMAPd. Overall, the ET times are in the picosecond regime and thereby markedly slower than the 50−150 fs time constants that we have reported for phenolphthalein and MGL.[25]

The structurally related molecules MGL and CVL are both set up around a tetrahedral carbon atom and are characterized by a nearly orthogonal arrangement of the electron-donating groups relative to the acceptor moiety. The structural difference between MGL and CVL—the presence of the amino group at the phthalide ring—results in a huge difference in the photophysics that has to be explained together with the observed dependence on the solvent.

IV.3. CVL Energetics and Population Transfer to the ^1CT_B State. In MGL, the optically excited state is localized on one of the dimethylamino groups, and the ET shifts the electron to the phthalide moiety. Because this ET proceeds on the time scale of vibrational motions in polar as well as nonpolar solvents, we can conclude that the CT state is already energetically accessible right after the excitation.

In nonpolar solvents, no ET is seen for CVL, and we can conclude that the optically excited ^1CT_A state (localized on the 6-DMAPd moiety) is lower than the ^1CT_B state that is delocalized over the whole molecule and similar in electronic structure to the CT state of MGL. For sufficiently polar solvents, the ET sets in, and we conclude that the solvation lowers the ^1CT_B state strongly enough to energetically allow the transfer and build up a significant population in the ^1CT_B state. A model that explicates this situation for the different steps during the solvation process is shown in Figure 7.

In the classical Marcus theory, the intramolecular coordinates relevant to the ET and the intermolecular coordinates of solvent distance and orientation are unified in a single generalized coordinate. Numerous time-resolved emission studies investigating solvation from an optically activated, nonequilibrated distribution clearly show that the emission band shifts with time and only changes its width to a smaller degree.[29,32,34] From this, it can be concluded that there is a separation of time scales between the intramolecular and pure solvation degrees of freedom, and it is meaningful to use two separate coordinates to describe the solvation of a single excited state.[33] The time-dependent spectral position of the emission band is equal to the momentary difference between the lowered excited-state energy and the rising ground-state energy. The width is given mainly by the Franck−Condon structure and the rapid solvent fluctuations and, to a lesser degree, by the inhomogeneous distribution of solvent environments. In this sense, we believe that it is appropriate in the investigated situation to use a quasi-two-dimensional description with one combined coordinate for the intramolecular degrees of freedom and the rapid fluctuations and a second slow solvation coordinate. The sketches in Figure 7 are to be understood as selected cross sections of this 2D potential energy surface for a given time and therefore extent of the solvation.

This picture of a single excited state has to be extended to the two excited states of CVL. Even in a highly polar solvent, the ^1CT_B state lies above the ^1CT_A state as long as the molecule is in the ground state with its low dipole moment and the

associated dynamic arrangement of the solvent molecules. The excitation of the ^1CT_A state instantaneously increases the molecular dipole moment and solvation, that is, the partial alignment of the polar solvent molecules, sets in. This lowers the ^1CT_A state but even more the highly polar ^1CT_B state with its similar localization of the negative charge. We therefore augment the sketches in Figure 7 by a second parabola for the ^1CT_B state with a time- (solvation) dependent crossing of the parabola describing the ^1CT_A state.

Eventually, the two CT states come close in energy, and assisted by the thermal fluctuations, the ET becomes possible. The strong electronic coupling in CVL that we infer from the 100 fs ET in the closely related MGL does then indeed lead to the ET. At this point in time, the reaction rates in forward and backward direction are equal. The ongoing solvation shifts the dynamic equilibrium between the ^1CT_A and ^1CT_B state toward the latter. The final equilibrium is established when the states are lowered from the initial energies by $E_S{}^A$ and $E_S{}^B$. The described interplay of the solvation and the ET leads to the experimentally observed solvent control of the ET, concerning both the extent and the speed.

IV.4. Modeling of the ET During Solvation. For a more quantitative description of the solvent-dependent ET, a suitable model has to be applied, and for this, a number of microscopic quantities have to be determined. We have to know the initial separation of the CT states and the total amount of energetic lowering (solvation energy) caused by each of the solvents. An estimate for the solvation times has to be accepted, and finally, the local heating has to be taken into account. The proper combination of these considerations leads to a knowledge of the energetics at each point in time and therefore allows the application of the Marcus theory[54,55] to determine a time-dependent ET rate.

Initial Separation of the CT States in Vacuum. As discussed in Section III.1, all of the CVL fluorescence originates from the ^1CT_A state for low polarity solvents and most from the ^1CT_B state for high polarity ones. Equal fluorescence decay times in both bands can be taken as an indication that the particular solvent leads to the equilibration of the two states at long times. Single intensive ($\Phi_{fl} = 0.44$) fluorescence in tetrahydrofuran ($\varepsilon = 7.6$) indicates the first case, and an intense second fluorescence band in the slightly more polar dichloromethane ($\varepsilon = 8.9$, total $\Phi_{fl} = 0.27$, $\tau_{fl} = 22.4$ ns in both the A and B bands) allows us to locate the ε value needed for the equilibration between these values. To estimate the separation of the CT states in vacuum, we start from the experimentally observed energetic situation in quasi-equilibrium, that is, after solvation, and then use calculated solvation energies to reconstruct the energetics of the isolated molecule.

For the calculation of the solvation energies $E_S{}^X$, we neglect the polarizability of the solute and use the Onsager solution for the dipolar reaction field:[56]

$$E_S{}^X = \frac{1}{4\pi\varepsilon_o}\frac{\mu_X{}^2}{a_X{}^3}\frac{\varepsilon-1}{2\varepsilon+1} \quad (1)$$

Here, a_X is the effective radius of the spherical Onsager cavity of the ^1CT_X state, its charge separation is represented by its dipole moment μ_X, and ε is the static dielectric constant of the solvent. For the ^1CT_A and ^1CT_B states of CVL, we use cavity radii of 3.6 and 5.8 Å, respectively,[57] and the experimentally determined values of the dipole moments of 10.7 and 25.2 D.[39] For the above-discussed situation of energetic equilibration after solvation (found between tetrahydrofuran and dichloromethane), the difference in solvation energies $\Delta E_S = E_S{}^B - E_S{}^A$ equals the sought energy gap without solvation.

ΔE_S rises from 1640 cm^{-1} in tetrahydrofuran to 1690 cm^{-1} in dichloromethane. From this, we estimate a value of $\Delta E_0^{vac} = 1660$ cm^{-1} for the separation of the ^1CT_A and ^1CT_B states in vacuum. We further identify the energy gap between the two states with the Gibbs free energy change ΔG^0 for the Marcus description of the CT.

Total Energetic Lowering Due to Solvation. For ACN, DMSO, and PC, the value of ΔE_S is determined at 1930, 1960, and 1970 cm^{-1}. These values lead to the conclusion that the ^1CT_B state is finally stabilized to $-\Delta G^0(t=\infty) = 270$, 300, and 310 cm^{-1} below the ^1CT_A state. Considering the thermal energy of about 200 cm^{-1} in the room temperature experiment, a nontrivial distribution between the states is reached according to

$$K_{eq} = \frac{[^1CT_B]}{[^1CT_A]} = \exp(-\Delta G^0/k_B T) \quad (2)$$

For ACN, this amounts to $K_{eq} = 3.86$, that is, an almost 4-fold larger population of the ^1CT_B state. The equilibrium persists until the electronic ground state is reached by back ET on the nanosecond time scale.[39]

Solvation Dynamics and Time-Dependent Energetics. The lowering of the two CT states and the establishment of the $^1CT_A \rightleftarrows {}^1CT_B$ equilibrium during solvation is a dynamic process. The energetics of educt and product are controlled by the dielectric relaxation properties of the solvent, as has been proposed for instance in the case of *t*-stilbene.[58] In detail, the energy separation of the states in vacuum ΔE_0^{vac} corrected for the difference $\Delta E_{S,el}$ of the instantaneous electronic part of the total solvation energy gives the initial energy separation $\Delta G^0(t=0)$ of the states in solution:

$$\Delta G^0(t=0) = \Delta E_0^{vac} - \Delta E_{S,el} = \Delta E_0^{vac} - \frac{1}{4\pi\varepsilon_o}\left(\frac{\vec{\mu}_B{}^2}{a_B{}^3} - \frac{\vec{\mu}_A{}^2}{a_A{}^3}\right)\frac{n^2-1}{2n^2+1} \quad (3)$$

Here, n is the refractive index of the solvent. The remaining part $\Delta E_{S,or} = \Delta E_S - \Delta E_{S,el}$ of the solvation energy, that is, the one due to the reorientation of the solvent molecules, is time dependent. The relevant time scales τ_i and amplitudes a_i in the different solvents can be taken from the known solvation parameters.[34] The Gibbs free energy change ΔG^0 for the ET can then be written as

$$\Delta G^0(t) = \Delta G^0(0) - \Delta E_{S,or}\left[1 - \sum_i a_i \exp(-t/\tau_i)\right] \quad (4)$$

We performed simulations of the time-dependent energy separation for ACN, DMSO, and PC and for comparison also for methanol. The results are shown in Figure 8a. For all four solvents, the energy gap crosses zero within at most a few picoseconds, corresponding to resonance between the two states. For ACN with its known fast solvation, this occurs already after a few 100 fs, for DMSO and for PC at about 1.5 ps. From this time on, the ET can proceed effectively. The relation of the stabilization capability $\Delta E_{S,or}$ to the initial energy gap $\Delta G^0(t=0)$ is the very reason why the solvent-controlled ET does not show the same time constants as the pure solvation. Methanol is included here to demonstrate the fact that an early ET can occur even in a solvent with slower reorganization.[59]

The description of the time-dependent change of the energy gap suggests a smooth and monotonic process. This is certainly

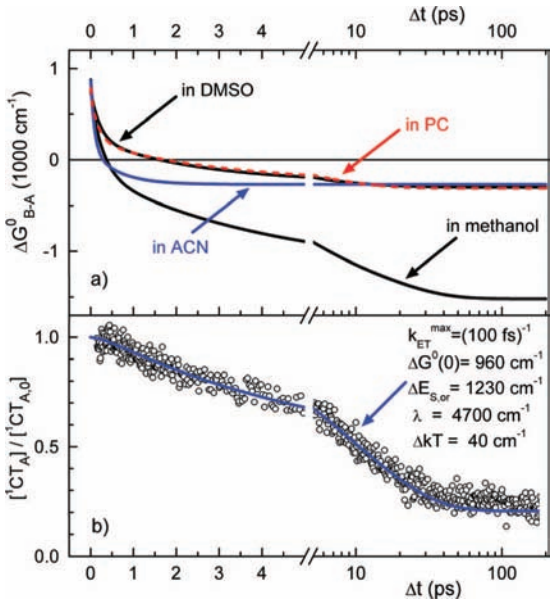

Figure 8. (a) Calculated change of the driving force $\Delta G^0(t)$ during the solvation process for the reaction from ^1CT_A to ^1CT_B for CVL in different solvents according to eq 4. (b) Normalized population of the ^1CT_A state (circles) in ACN after 370 nm excitation obtained from the kinetic curve at 470 nm probe wavelength (see Figure 7 upper curve). The solid line shows the simulation of the ^1CT_A population according to the kinetic model described in the text (eqs 5 and 6).

only a crude approximation because only a quasi-equilibrium can be expected at any point in time. The solvation is actually accomplished via statistical fluctuations of the solvent polarization around the average.[60] Occasionally, an arrangement of solvent molecules will occur that will equate the energies of the ^1CT_A and ^1CT_B states enabling the ET.

Application of Marcus Theory. Equation 4 implies that the reaction barrier for ET becomes time dependent and consequently also the ET rate. Time-dependent reaction barriers have been proposed for instance by Simon[61] for solvent nonequilibrated ET processes and for photoisomerization reactions by Mohrschladt et al.[62] To model the overall process, we apply the Marcus theory with the time-dependent driving force from eq 4 and the reorganization energy λ:

$$k_{ET}(t) = k_{ET}^{max} \exp\left(\frac{-(\lambda \pm \Delta G^0(t))^2}{4\lambda k_B T}\right) \qquad (5)$$

The plus sign refers to the forward and the minus sign to the backward ET. k_{ET}^{max} is the preexponential factor that gives an upper limit for the ET in the case of a vanishing barrier. It is determined by the electronic coupling. Because of the similarity of MGL and CVL, we adapt the experimental value of (100 fs)$^{-1}$ found for MGL for the present study on CVL.

With the time-dependent ET rates given by eq 5, we numerically determine the time dependence of the population of the two CT states. The forward and backward reaction rates are explicitly considered via the usual equation:

$$\frac{d[^1CT_A]}{dt} = -k_{ET}^{+}(t)[^1CT_A] + k_{ET}^{-}(t)(1 - [^1CT_A]) \qquad (6)$$

This result can be directly compared to the experimental recordings if we normalize the experimental data to the initial population of the ^1CT_A state. A typical result for the depopulation of the ^1CT_A state is shown in Figure 8b. The small offset at long times is due to the persistent equilibrium population discussed above. It is important to note that all kinetic information used in the model is taken from independent experiments. The time constants given in Table 1 did not enter the final model and have to be regarded as rough indications of the relevant time scales only.

For the good agreement between modeling and experiment, two further details were important. First, the value of λ had to be adjusted to match the observation at long times. The value of 4700 cm^{-1} is in a typical range for comparable systems.[63,64] We can also compare this value to the reorganization contribution of the solvent which can be estimated according to a derivation by Marcus[55] to 4470 cm^{-1}.[65] As expected for a solvation-controlled reaction, the intramolecular component plays only a minor role.

Second, we noticed that the assumption of a constant temperature did not allow the desired quality of the modeling. It is reasonable to assume that the molecule is slightly heated because of the optical excitation that includes some vibrational excess energy. Because of the optical selection rules and the fact that the internal vibrational redistribution is far from complete within the first picosecond, a highly nonstatistical distribution has to be assumed. Accordingly, the temperature in relevant modes can easily deviate from the limited value that one would calculate from full statistics. The increase in local temperature (corresponding to an empirical value of 40 cm^{-1}, in good agreement with ref 66) will decay exponentially on a picosecond time scale. We used reported cooling times for ACN[67] to derive the time-dependent temperature $k_B T(t) = [200 + 40(0.6\ e^{-t/2.6\ ps} + 0.4\ e^{-t/11\ ps})]$ cm^{-1}.

At the moment, the model does not allow for a precise and detailed prediction of the solvent driven ET dynamics because the applied values of several parameters are rough estimations and the obtained dynamics is quite sensitive to these values. However, the good agreement between the modeled and the measured time-dependent CT populations demonstrates that it reflects the key features of the dynamics. They result from the variation of the ET rate with time because of the changes of the CT energetics caused by the ongoing solvation.

Strictly speaking, the Marcus theory was originally formulated for a quasi-equilibrium situation. In the situation discussed in this work, this condition is only fulfilled marginally because the intrinsic ET rate is somewhat faster than the solvation. Sumi and Marcus expanded the theory to dynamical effects and derived algebraic formulas to describe this more complicated situation.[68] However, because of the various additional contributions to the spectroscopic observations and the limited applicability of simple analytic ET models,[69] we presently restrain ourselves from the direct application of such formalisms. In future work, full molecular dynamics simulations[70,71] incorporating modern analytic aspects[72,73] should be used to model the combined solvation and ET dynamics without artificial separation of coordinates and time scales.

V. Conclusions

The photophysics of CVL are strongly influenced by the surrounding medium. The solvent polarity dynamically determines the energetics of both CT states and controls the availability of the various deactivation pathways. In this work, we focused on the effect that the solvation dynamics has on the photoinduced ET reaction in CVL and addressed the question of how it enables and controls ET. In a fs pump−probe study of the CVL photophysics in solvents of different polarity, we found a strong connection between the solvation dynamics and the observable $^1CT_A \rightarrow {}^1CT_B$ population transfer. The ^1CT_B state

is populated with a time-dependent rate, and the observed CT dynamics is significantly affected by the competition between solvent relaxation and reaction. In ionic solvents, it has recently been found that the ET of CVL shows strong environmental heterogeneity[74] instead of the temporal evolution found by us for the polar organic solvents.

We used TA measurements instead of the more usual time-resolved emission. At least for the present case of CVL, TA proves to be a very sensitive and informative probe for the CT process. We want to point out that TA spectroscopy has already been used by others quite successfully to even study solvation without any additional reactive process.[33]

Even though it might seem trivial, the energetic position of the educt and product is not explicitly treated in many of the theoretical and experimental studies concerning the solvent-controlled ET regime. It can, however, explain the strong variation of time constants attributed to solvation-controlled ET in different molecular systems in a straightforward fashion. These time constants cannot be uniformly correlated to the solvation dynamics because the energetics between donor and acceptor vary with the molecular systems. Similarly, the theoretical approaches only consider the influence of the solvent on the preexponential factor and implicitly assume the energetic configuration to be independent of time.[68,75] The experimental findings in CVL clearly show that it is not only the solvation dynamics that is decisive for the control of the ET but also the amount of stabilization that is achieved on a certain time scale. Without sufficient energetic stabilization of the product state, no ET is found at all.

We believe that the present results and conclusions are relevant for a wide range of spiro-like donor−acceptor molecules with one bond mediating an ultrafast intramolecular ET process. For a large body of spiro-type molecules with both theoretical and practical relevance, such as, for example, photochromic spiropyranes and spirooxazines, CVL can be considered as a molecule that visualizes the CT processes underlying their photophysics and photochemistry.

The formation of the ^1CT_B state from the ^1CT_A is due to ET from the DMA group to the 6-DMAPd subunit with formation of an intramolecular exciplex. Directly after optical excitation, the energy separation is so large that we suggest to call the ET nonadiabatic at this early time. When the lowering of both states due to solvation leads to energetic equilibration, the ET turns into an adiabatic reaction.[75] The latter situation resembles the ET processes occurring faster than diffusive solvation both in intra-[7] and in intermolecular[63,76−78] CT reactions involving dimethylaniline as electron donor. Both CVL and the related MGL offer a number of advantages and may be used as model systems in controversies concerning ET rates[17,78] in such systems. In both LTAMs, the electron donor is in direct contact (via a covalent bond) with the acceptor, so that no diffusional translation and reorientation is needed to induce ET. The ET process proceeds intramolecularly in a well-defined geometry, allowing one to study the ET kinetics and dynamics with only one mutual donor−acceptor orientation and distance. The experimental findings will consequently be much more directly comparable to theoretical studies without the need for extensive averaging.

Acknowledgment. Financial support from Grant 3T09A06929 from the Polish Ministry of Science and Higher Education and European Community Grant G5MA-CT-2002-04026 (J.K.) and The International Max Planck Research School on Advanced Photon Science (U.M.) is gratefully acknowledged. The collaboration was supported by a travel grant from the Deutsche Forschungsgemeinschaft and by the SFB 749 (Dynamik und Intermediate molekularer Transformationen).

References and Notes

(1) Bagchi, B.; Gayathri, N. *Adv. Chem. Phys.* **1999**, *107*, 1.
(2) Zusman, L. D. *Chem. Phys.* **1980**, *49*, 295.
(3) For a review see Jortner; J.; Bixon, M., Eds. Electron transfer: from isolated molecules to biomolecules. *Adv. Chem. Phys.*; J. Wiley: New York 1999; Vols. *106−107*.
(4) Weaver, M. J. *Chem. Rev.* **1992**, *92*, 463.
(5) (a) Kang, T. J.; Kahlow, M. A.; Giser, D.; Swallen, S.; Nagarajan, V.; Jarzęba, W.; Barbara, P. F. *J. Phys. Chem.* **1988**, *92*, 6800. (b) Kang, T. J.; Jarzęba, W.; Barbara, P. F.; Fonseca, T. *Chem. Phys.* **1990**, *149*, 81. (c) Tominaga, K.; Walker, G. C.; Kang, T. J.; Barbara, P. F.; Fonseca, T. *J. Phys. Chem.* **1991**, *95*, 10485.
(6) Horng, M. L.; Dahl, K.; Jones, G., II.; Maroncelli, M. *Chem. Phys. Lett.* **1999**, *315*, 363.
(7) Tominaga, K.; Walker, G. C.; Jarzęba, W.; Barbara, P. F. *J. Phys. Chem.* **1991**, *95*, 10475.
(8) Barthel, E. R.; Martini, I. B.; Schwartz, B. J. *J. Phys. Chem. B* **2001**, *105*, 12230.
(9) Saleh, N.; Kauffman, J. F. *J. Phys. Chem. A* **2004**, *108*, 7139.
(10) Glasbeek, M.; Zhang, H. *Chem. Rev.* **2004**, *104*, 1929.
(11) Grabowski, Z. R.; Rotkiewicz, K.; Rettig, W. *Chem. Rev.* **2003**, *103*, 3899.
(12) Kosower, E. M.; Huppert, D. *Annu. Rev. Phys. Chem.* **1986**, *37*, 127.
(13) Kahlow, M. A.; Kang, T. J.; Barbara, P. F. *J. Phys. Chem.* **1987**, *91*, 6452.
(14) Kobayashi, T.; Takagi, Y.; Kandori, H.; Kemnitz, K.; Yoshihara, K. *Chem. Phys. Lett.* **1991**, *180*, 416.
(15) Pöllinger, F.; Heitele, H.; Michel-Beyerle, M. E.; Anders, C.; Fuscher, M.; Staab, H. A. *Chem. Phys. Lett.* **1992**, *198*, 645.
(16) Walker, G. C.; Åkesson, E.; Johnson, A. E.; Levinger, N. E.; Barbara, P. F. *J. Phys. Chem.* **1992**, *96*, 3728.
(17) Baigar, E.; Gilch, P.; Zinth, W.; Stöckl, M.; Härter, P.; von Feilitzsch, T.; Michel-Beyerle, M. E. *Chem. Phys. Lett.* **2002**, *352*, 176.
(18) Son, D. H.; Kambhampati, P.; Kee, T. W.; Barbara, P. F. *J. Phys. Chem. A* **2002**, *106*, 4591.
(19) Mataga, N.; Chosrowjan, H.; Taniguchi, S.; Shibata, Y.; Yoshida, N.; Osuka, A.; Kikuzawa, T.; Okada, T. *J. Phys. Chem. A* **2002**, *106*, 12191.
(20) Giaimo, J. M.; Gusev, A. V.; Wasielewski, M. R. *J. Am. Chem. Soc.* **2002**, *124*, 8530.
(21) Yoshihara, K.; Yartsev, A.; Nagasawa, Y.; Kandori, H.; Douhal, A.; Kemnitz, K. *Pure Appl. Chem.* **1993**, *65*, 1671.
(22) Iwai, S.; Murata, S.; Tachiya, M. *J. Chem. Phys.* **1998**, *109*, 5963.
(23) (a) Jortner, J.; Bixon, M.; Heitele, H.; Michel-Beyerle, M. E. *Chem. Phys. Lett.* **1992**, *197*, 131. (b) Bixon, M.; Jortner, J. *J. Phys. Chem.* **1993**, *97*, 13061.
(24) Bixon, M.; Jortner, J. *Adv. Chem. Phys.* **1999**, *106*, 35.
(25) Bizjak, T.; Karpiuk, J.; Lochbrunner, S.; Riedle, E. *J. Phys. Chem. A* **2004**, *108*, 10763.
(26) Kovalenko, S. A.; Pérez Lustres, J. L.; Ernsting, N. P.; Rettig, W. *J. Phys. Chem. A* **2003**, *107*, 10228.
(27) Kubo, M.; Mori, Y.; Otani, M.; Murakami, M.; Ishibashi, Y.; Yasuda, M.; Hosomizu, K.; Miyasaka; H.Imahori, H.; Nakashima, S. *J. Phys. Chem. A* **2007**, *111*, 5136.
(28) Rosenthal, S. J.; Xie, X.; Du, M.; Fleming, G. R. *J. Chem. Phys.* **1991**, *95*, 4715.
(29) Maroncelli, M. *J. Mol. Liq.* **1993**, *57*, 1.
(30) Barbara, P. F.; Jarzęba, W. *Adv. Photochem.* **1990**, *15*, 1.
(31) Jimenez, R.; Fleming, G. R.; Kumar, P. V.; Maroncelli, M. *Nature* **1994**, *369*, 471.
(32) Ruthmann, J.; Kovalenko, S. A.; Ernsting, N. P.; Ouw, D. *J. Chem. Phys.* **1998**, *109*, 5466.
(33) Pérez Lustres, J. L.; Kovalenko, S. A.; Mosquera, M.; Senyushkina, T.; Flasche, W.; Ernsting, N. P. *Ang. Chem., Int. Ed.* **2005**, *44*, 5635.
(34) Horng, M. L.; Gardecki, J. A.; Papazyan, A.; Maroncelli, M. *J. Phys. Chem.* **1995**, *99*, 17311.
(35) Åkesson, E.; Walker, G. C.; Barbara, P. F. *J. Chem. Phys.* **1991**, *95*, 4188.
(36) Londergan, C. H.; Salsman, J. C.; Ronco, S.; Dolkas, L. M.; Kubiak, C. P. *J. Am. Chem. Soc.* **2002**, *124*, 6236.
(37) Wang, Ch.; Mohney, B. K.; Akhremitchev, B. B.; Walker, G. C. *J. Phys. Chem. A* **2000**, *104*, 4314.
(38) Martini, I. B.; Barthel, E. R.; Schwartz, B. J. *Science* **2001**, *293*, 462.
(39) Karpiuk, J. *J. Phys. Chem. A* **2004**, *108*, 11183.
(40) Karpiuk, J.; Karolak, E.; Nowacki, J. *Pol. J. Chem.* **2008**, *82*, 865.
(41) Karpiuk, J. *Phys. Chem. Chem. Phys.* **2003**, *5*, 1078.
(42) Karpiuk, J.; Grabowski, Z. R.; De Schryver, F. C. *J. Phys. Chem.* **1994**, *98*, 3247.

(43) Fischer, O. *Chem. Ber.* **1879**, *12*, 1685.
(44) Stanetty, P.; Rodler, I.; Krumpak, B. *J. prakt. Chem.* **1993**, *335*, 17.
(45) Duxbury, D. F. *Chem. Rev.* **1993**, *93*, 381.
(46) Nagasawa, Y.; Ando, Y.; Kataoka, D.; Matsuda, H.; Miyasaka, H.; Okada, T. *J. Phys. Chem. A* **2002**, *106*, 2024.
(47) Kuzuya, M.; Miyake, F.; Okuda, T. *Chem. Pharm. Bull.* **1983**, *31*, 791.
(48) Jarikov, V. V.; Neckers, D. C. *Adv. Photochem.* **2001**, *26*, 1, and references cited therein.
(49) Karpiuk, J.; Svartsov, Y. N.; Nowacki, J. *Phys. Chem. Chem. Phys.* **2005**, *7*, 4070.
(50) Marcus, R. A. *J. Phys. Chem.* **1989**, *93*, 3078.
(51) The values of $\mu_e = 11.2$ D derived from a steady-state solvatochromic study and of the angle between $\vec{\mu}_e$ and $\vec{\mu}_g$ (34.8°) used here differ from those published earlier (ref 39) for 6-DMAPd (9.7 D, 32°) because of different μ_g values assumed (5.9 D from AM1 calculations in ref 39 instead of 6.55 D in ref 49 from the DFT method).
(52) Shida, T. *Electronic absorption spectra of radical ions*; Elsevier: New York, 1988.
(53) De Waele, V.; Beutter, M.; Schmidhammer, U.; Riedle, E.; Daub, J. *Chem. Phys. Lett.* **2004**, *390*, 328.
(54) Marcus, R. A. *J. Chem. Phys.* **1956**, *24*, 966.
(55) Marcus, R. A.; Sutin, N. *Biochim. Biophys. Acta* **1985**, *811*, 265.
(56) Onsager, L. *J. Am. Chem. Soc.* **1936**, *58*, 1486.
(57) The choice of different Onsager radii for both CT states has been discussed in detail in ref 39.
(58) Hicks, J. M.; Vandersall, M. T.; Sitzmann, E. V.; Eisenthal, K. B. *Chem. Phys. Lett.* **1987**, *135*, 413.
(59) In protic solvents, the solvation (as overall stabilization resulting from interactions with the solvent) of CVL comprises a contribution due to hydrogen bonding.
(60) Calef, D. F.; Wolynes, P. G. *J. Phys. Chem.* **1983**, *87*, 3387.
(61) Simon, J. D. *Pure Appl. Chem.* **1990**, *62*, 2243.
(62) Mohrschladt, R.; Schroeder, J.; Schwarzer, D.; Troe, J.; Vöhringer, P. *J. Chem. Phys.* **1994**, *101*, 7566.
(63) Nad, S.; Pal, H. *J. Phys. Chem. A* **2000**, *104*, 673.
(64) Nad, S.; Pal, H. *J. Chem. Phys.* **2002**, *116*, 1658.
(65) For a bimolecular ET reaction with a given distance r_{DA} between a spherical donor (r_D) and acceptor (r_A), the reorganization energy is given by $\lambda_O = e^2/4\pi\varepsilon_0[1/(2r_D) + 1/(2r_A) - 1/r_{DA}](1/n^2 - 1/\varepsilon)$. Here, n and ε are the refractive index and dielectric constant of the solvent, respectively. In analogy to ref 39, we used $r_D = 3$ Å, $r_A = 3.6$ Å, and $r_{DA} = 4.3$ Å.
(66) Maroncelli, M. *J. Chem. Phys.* **1991**, *94*, 2084.
(67) Kovalenko, S. A.; Schanz, R.; Hennig, H.; Ernsting, N. P. *J. Chem. Phys.* **2001**, *115*, 3256.
(68) Sumi, H.; Marcus, R. A. *J. Chem. Phys.* **1986**, *84*, 4894.
(69) Barbara, P. F.; Walker, G. C.; Smith, T. P. *Science* **1992**, *256*, 975.
(70) Hilczer, M.; Tachiya, M. *J. Mol. Liq.* **2000**, *86*, 97.
(71) Scherer, P. O. J.; Tachiya, M. *J. Chem. Phys.* **2003**, *118*, 4149.
(72) Denny, R. A.; Bagchi, B.; Barbara, P. F. *J. Chem. Phys.* **2001**, *115*, 6058.
(73) Burghardt, I.; Bagchi, B. *Chem. Phys.* **2006**, *329*, 343.
(74) Jin, H.; Li, X.; Maroncelli, M. *J. Phys. Chem. B* **2007**, *111*, 13473.
(75) Gladkikh, V.; Burshtein, A. I. *J. Phys. Chem. A* **2005**, *109*, 4983.
(76) Yoshihara, K.; Tominaga, K.; Nagasawa, Y. *Bull. Chem. Soc. Jpn.* **1995**, *68*, 696.
(77) Castner, E. W., Jr.; Kennedy, D.; Cave, R. J. *J. Phys. Chem. A* **2000**, *104*, 2869.
(78) Morandeira, A.; Fürstenberg, A.; Gumy, J.-C.; Vauthey, E. *J. Phys. Chem. A* **2003**, *107*, 5375.

JP800863U